

Comparison of different tissue clearing methods and 3D imaging techniques for visualization of GFP-expressing mouse embryos and embryonic hearts

Hana Kolesová¹ · Martin Čapek² · Barbora Radochová² · Jiří Janáček² · David Sedmera^{1,2}

Accepted: 20 April 2016 / Published online: 4 May 2016
© Springer-Verlag Berlin Heidelberg 2016

Abstract Our goal was to find an optimal tissue clearing protocol for whole-mount imaging of embryonic and adult hearts and whole embryos of transgenic mice that would preserve green fluorescent protein GFP fluorescence and permit comparison of different currently available 3D imaging modalities. We tested various published organic solvent- or water-based clearing protocols intended to preserve GFP fluorescence in central nervous system: tetrahydrofuran dehydration and dibenzylether protocol (DBE), SCALE, CLARITY, and CUBIC and evaluated their ability to render hearts and whole embryos transparent. DBE clearing protocol did not preserve GFP fluorescence; in addition, DBE caused considerable tissue-shrinking artifacts compared to the gold standard BABB protocol. The CLARITY method considerably improved tissue transparency at later stages, but also decreased GFP fluorescence intensity. The SCALE clearing resulted in sufficient tissue transparency up to ED12.5; at later stages the useful depth of imaging was limited by tissue light scattering. The best method for the cardiac specimens proved to be the CUBIC protocol, which preserved GFP fluorescence well, and cleared the specimens sufficiently even at the adult stages. In addition, CUBIC decolorized the blood and myocardium by removing tissue iron. Good 3D

renderings of whole fetal hearts and embryos were obtained with optical projection tomography and selective plane illumination microscopy, although at resolutions lower than with a confocal microscope. Comparison of five tissue clearing protocols and three imaging methods for study of GFP mouse embryos and hearts shows that the optimal method depends on stage and level of detail required.

Keywords Green fluorescent protein (GFP) · Confocal microscopy · Optical projection tomography · Tissue transparency · Heart · Embryo

Introduction

Recent advances in molecular genetics have resulted in a plethora of animal models expressing fluorescent proteins in various tissues and organs. Unlike the previous generation of markers such as LacZ, which require substrates to visualize their expression, fluorescent proteins, such as green fluorescent protein (GFP), can be observed directly in vivo using epifluorescence microscopy. Depth of imaging is limited by tissue opacity and light penetration. The original tissue clearing protocols based upon organic solvents enabling light penetration deep into the sample did not preserve GFP fluorescence (Zucker et al. 1998). Insufficient GFP fluorescence preservation could be overcome by using whole-mount immunohistochemistry followed by tissue clearing with benzyl alcohol:benzyl benzoate (BABB) mix (e.g., Miller et al. 2005; Sankova et al. 2012), but this approach first negates the advantage of direct visualization of the fluorescent reporter and, second, introduces another potential problem with imperfect antibody penetration.

To overcome these limitations, several methods of tissue clearing were developed, mainly by the investigators

Electronic supplementary material The online version of this article (doi:10.1007/s00418-016-1441-8) contains supplementary material, which is available to authorized users.

✉ David Sedmera
david.sedmera@lf1.cuni.cz

¹ Institute of Anatomy, First Faculty of Medicine, Charles University in Prague, U Nemocnice 3, 128 00 Prague 2, Czech Republic

² Institute of Physiology, The Czech Academy of Sciences, 142 20 Prague, Czech Republic

studying the central nervous system, where tracking of small nerve processes over large distance in three dimensions is highly desirable. Since all these techniques are optimized for the nervous tissue, which differs significantly from the heart specimens (high fat content, relative lack of autofluorescence), in this study we compared five preservation protocols on embryonic and adult cardiac tissue.

The first method tested relies on dehydration of the specimens using tetrahydrofuran (THF) followed by their clearing in dibenzylether (DBE) (Becker et al. 2012). Second method tested is named CLARITY and uses electrophoretic lipid washout after cross-linking the samples in polyacrylamide gels (Chung et al. 2013). Third tested method is called SCALE, and its water-based protocols include glycerol, Triton X-100 and high concentration (4 M) aqueous urea (Hama et al. 2011) or saturated fructose solution (Ke et al. 2013). The last tested tissue clearing method is a modified SCALE protocol supplemented with N,N,N,N-tetrakis(2-hydroxypropyl)ethylenediamine named CUBIC (Tainaka et al. 2014). All protocols were compared to standard tissue clearing protocol BABB. In all tissue clearing methods preservation or bleaching of GFP fluorescence was tested as well as depth of tissue clearing in different embryonal developmental stages and in different tissues (head vasculature, coronary arteries, superficial and deep heart structures).

The test of five tissue clearing methods for cardiac tissue was combined with a test of four different imaging methods. Reasons for 3D-visualization and cardiac tissue imaging are multiple, including tracking of the coronary artery tree (Hu et al. 2000), evaluating myofiber orientation (Jouk et al. 2000) or visualization of the cardiac conduction system (Ryu et al. 2009), allowing to study the three-dimensional network used for electrical impulse propagation. In this study, we compared widely used imaging methods, single-photon and multi-photon confocal microscopy with optical projection tomography (OPT) and selective plane illumination microscopy (SPIM), and evaluated their use to study cardiac development. OPT was successfully recently used in combination with BABB clearing to quantify infarction size in adult mouse heart (Zhao et al. 2015), while use of SPIM for cardiac system development is tested for the first time in this study.

Two transgenic mouse models expressing GFP in the heart were used to evaluate preservation and visualization of GFP signal. The Connexin40-GFP knock-in mice (Miquerol et al. 2004) highlight the cardiac conduction system and arterial tree, and the Nkx2.5:GFP knock-in mice (Biben et al. 2000) selectively label the myocardium and later show enhancement in the conduction tissues.

We seek to develop non-destructive tissue clearing and 3D imaging method of embryonic heart samples to study the atria and ventricles during the development as well as

differentiating Purkinje fiber network. Here we report on relative advantages and disadvantages of different GFP-preserving tissue clearing protocols and 3D imaging methods in mouse cardiac samples of different developmental stages.

Materials and methods

Animals

Cx40:GFP knock-in mice were described previously (Miquerol et al. 2004). Mice were maintained in a homozygous state and crossed with the wild-type strain to produce heterozygous embryos. Cx40:GFP heterozygous embryos do not have any heart malformations as previously reported in the Connexin40-null mice (Simon et al. 1998). The noon of the day when vaginal plug was discovered was considered embryonic day (ED)0.5. Time-pregnant females were killed by cervical dislocation, and the embryos at desired stages (ED10.5–ED18.5) rapidly dissected and perfusion-fixed (Sedmera et al. 1997) in 4 % (wt/vol) paraformaldehyde for 48 h. After fixation and thorough rinsing in phosphate buffer saline (PBS), the embryos or isolated hearts were treated according to tissue clearing protocols detailed below. All applicable international, national and institutional guidelines for the care and use of animals were followed. All procedures performed on animals were in accordance with the ethical standards of the Charles University in Prague and were approved by the Animal Care and Use Committee of the First Faculty of Medicine.

Clearing protocols

For clearing the mouse embryos and hearts various published organic solvent- or water-based clearing protocols claiming to preserve GFP fluorescence in central nervous system were used: tetrahydrofuran dehydration and DBE clearing (Becker et al. 2012), SCALE (Hama et al. 2011), CLARITY (Chung et al. 2013) and CUBIC (Tainaka et al. 2014), and their ability to render hearts and whole embryos transparent was evaluated. For comparison of the clearing ability 50 % (wt/vol) benzyl alcohol/50 % (wt/vol) benzyl benzoate (BABB), also known as Murray's clear, was used as a standard (Miller et al. 2005; Zucker et al. 1998), even though it does not preserve GFP fluorescence.

DBE

After fixation, the embryos and hearts were dehydrated using ascending THF series followed by clearing in DBE exactly as described (Becker et al. 2012), including all the precautions (filtration through aluminum oxide, monitoring of epoxides).

CLARITY

The protocol was originally described in (Chung et al. 2013). The specimens in phosphate buffer saline (PBS) were first soaked in and then embedded into de-gassed 4 % (wt/vol) bis-acrylamide (BioRad). Polymerization was initialized by addition of ammonium persulfate. Gel blocks were then subjected to 5 days of electrophoretic clearing in circulating borate buffer (pH 8.5), followed by additional clearing in SCALE for 1 week and imaging in SCALE.

SCALE

The protocol was initially described in Hama et al. (2011) as *SCALEA2*, here referred to as SCALE. The SCALE solution consists of 4 M urea, 10 % (wt/vol) glycerol and 0.1 % (wt/vol) Triton X-100, all in distilled water. Specimens were cleared in several changes of SCALE according to the developmental stage for 7–14 days at the room temperature. Longer stay in SCALE (beyond 2 weeks) did not improve the clearing. Embryos and hearts were subsequently stored at 4 °C before evaluation.

CUBIC

This protocol was originally described in Tainaka et al. (2014) for the brain specimens. Specifically, protocol described as SCALE/CUBIC-1 was used here, referred to as CUBIC. CUBIC solution contains 25 % (wt/vol) of urea, 25 % (wt/vol) of N,N,N,N-tetrakis(2-hydroxypropyl)ethylenediamine and 15 % (wt/vol) polyethylene glycol mono-p-isooctylphenyl ether (Triton X-100) in water. Components of CUBIC need to be thoroughly mixed for 30 min at 37 °C and stored at room temperature. Specimens were immersed in the CUBIC solution and gently rocked at 37 °C. CUBIC solution was changed every 3–4 days. After clearing, the specimens were stored in CUBIC at the 4 °C and prior to microscopic imaging transferred to SCALE.

All chemicals were obtained from Sigma (Prague, Czech Republic) except for glycerol and urea (obtained from Penta, Brno, Czech Republic) and Triton X-100 (Roth, Karlsruhe, Germany).

Imaging

Single-photon confocal microscopy

High-resolution images were obtained with single-photon confocal system FluoView FV1000 fitted on an upright BX61 microscope (Olympus, Tokyo, Japan), using 4× (NA 0.16, WD 13 mm) and 10× (NA 0.40, WD 3.1 mm) dry, 25× (NA 1.0, WD 4.0 mm) ScaleView dipping objective and 40× oil immersion (NA 1.30, WD 0.2 mm) lens using

appropriate filter sets for GFP (488 nm excitation) and autofluorescence (543 nm). Specimens, where nuclei were stained in whole mount with Hoechst 33342 dye, were also imaged at 405-nm excitation. Z-step varied between 0.5 and 25 μm, according to the objective lens. All pictures presented from a single-photon confocal microscope were photographed from non-sectioned whole embryos and hearts. Whole embryos were imaged in custom-made chambers (Petri dishes of different sizes with cast silicone bottom glued to a specimen slide). For embryos up to ED12.5 and for the isolated hearts cavity slides with coverslip were used (Fisher Scientific, Pittsburgh, PA). Photographs with the Z-stack were assembled in ImageJ (NIH, Bethesda, MD, USA).

Macrophotography

Whole embryos were photographed under a dissecting microscope (Olympus SZX, Tokyo, Japan) in a glass Petri dish without coverslip in the respective clearing media using Olympus DP50 CCD camera.

Multi-photon microscopy

GFP fluorescence was elicited at 950 nm in a two-photon mode during demonstration of the ScaleView lens at the Technical University, Munchen, Germany, on an upright Olympus fixed-stage confocal system. Z-series spanning 1 mm distance were collected at 1-μm steps at 512 × 512 pixels, resulting in voxels of 1 μm³ volume size.

Optical projection tomography (OPT). OPT is an imaging platform for studying microstructures in 3D (Sharpe et al. 2002). The method requires the tissue to be optically cleared to allow light to pass through the object. It is based on acquiring sets of optical projections of the specimen within a scope of view of 360° and the subsequent calculating of the 3D image using tomographic reconstruction. The principle is therefore similar to computed tomography, but instead of X-rays OPT uses visible light for demonstration of cleared tissues. Prior to visualization either by OPT or by SPIM, specimens have to be embedded in a block of agarose. Afterward, the agarose is glued by Super-glue to a specimen holder. To adapt refractive indices, the blocks are immersed into a cuvette with solution that was used for clearing the specimen or in SCALE in case of CLARITY. Data acquired by OPT are preprocessed to correct for optical axis mismatches, possible movements of the agarose blocks due to specimen weight (important for large embryos), and reconstructed. Alignment was complete in case of acquisition of multiple channels. For acquisition of specimens we used primarily a custom-made OPT machine that was developed in cooperation with the Politecnico di Milano, Italy (see <http://www.fisi.polimi.it/>)

[en/research/research_structures/laboratories/50528](#)) and installed in the Institute of Physiology, Czech Academy of Sciences in Prague (Cvetko et al. 2015). The custom-made OPT machine is equipped with a more sensitive camera and more precise PlanApo long working distance infinity-corrected dry objectives (Edmund Optics, Barrington, NJ, USA), providing thus images of higher quality than the commercial system below. We used objective lens 2× (NA 0.055), 5× (NA 0.14) and 10× (NA 0.28) that cover fields of view $5.5 \times 5.5 \text{ mm}^2$, $2.2 \times 2.2 \text{ mm}^2$ and $1.1 \times 1.1 \text{ mm}^2$, respectively. Second, for larger specimens such as the whole embryos, we used the commercial OPT 3001 scanner made by Bioptonics (Edinburgh, UK) having lower image quality but zoomable optics suitable for adapting the larger specimens to the field of view (<http://bioptonics.co.uk>).

The specimens were acquired using an excitation wavelength of 405 nm and emission wavelengths from 550 nm with a high-pass filter. For every specimen, 400 image projections, obtained with a step of 0.9 degrees, were captured at 16 bits per pixel. Three-dimensional reconstructions were created using NRecon, a free software package available online (<http://www.skyscan.be/products/downloads.htm>). The resolutions of full 3D reconstructed images were 512^3 (Bioptonics) or 1024^3 voxels (Milano), with the voxel sizes depending on the used magnification and objectives starting with the value of $1.13 \mu\text{m}^3$.

Selective plane illumination microscopy (SPIM)

The SPIM is based on noninvasive optical sectioning of a cleared fluorescing specimen by focusing a thin laser light sheet and taking two-dimensional images of the illuminated slice with a perpendicularly positioned CCD camera. Three-dimensional stacks are obtained by moving the specimen perpendicularly to the light sheet. We constructed an SPI microscope according to the OpenSPIM project—openspim.org (Pitrone et al. 2013), and the machine is installed in the Institute of Physiology, Czech Academy of Sciences.

We imaged the specimens using a 10× water dipping objective (NA 0.3, WD 3.5 mm) coupled with a 0.63× magnifying camera mount giving the resulting magnification of 6.3×, allowing us to capture specimens having the maximum size of $1.3 \times 1.3 \times 3.5 \text{ mm}$ in a single field of view, or more with image tiling and specimen flipping. For illumination of the specimens we used Coherent Cube laser with excitation at 490 nm. Emission light corresponding to GFP was captured using the emission band-pass filter 502/35 nm (Chroma, Bellows Falls, VT, USA). The detector was an Andor iXon3 EM-CCD camera (Andor, Belfast, UK) with 12-bit pixel depth and 512×512 sensor resolution. The Z-step was set to 6 μm , and the number of sections varied from 100 to 350.

Results

In our study we evaluated and compared several tissue clearing protocols. The aim was to find a method, which would clear sufficiently the tissue for confocal microscopy, OPT and SPIM, while also being able to preserve GFP fluorescence in transgenic mouse tissues.

The first method tested was the DBE tissue clearing protocol, which despite the careful control of all critical parameters was not able to preserve GFP fluorescence. In addition, it caused considerable tissue shrinking and deformations (worse than BABB, Fig. 1).

To further enhance tissue transparency, we tested the CLARITY electrophoretic tissue clearing protocol (Chung et al. 2013). CLARITY compared well to the following methods based upon chemical tissue clearing, and the only improvement was noted in older specimens (ED18.5 and adult). However, while the tissue transparency was sufficient, CLARITY decreased or entirely eliminated GFP fluorescent signal from embryos (data not shown). The only sample, where CLARITY was able to preserve GFP signal, was the adult heart, where we observed GFP-positive coronary artery endothelium in the interventricular septum (Fig. 4). Therefore, the CLARITY method is suitable for preserving GFP fluorescence in adult hearts only.

The third method tested was the SCALE protocol according to Hama et al. (2011). This protocol, unlike previous methods, was able to preserve GFP fluorescence, and it also resulted in reasonable tissue clearing (Fig. 1). However, while SCALE cleared well small whole embryos that were observed with confocal microscope, only the hearts and embryos up to ED12.5 were sufficiently transparent (Fig. 2). In older embryonic hearts the area and depth of imaging were limited by significant tissue light scattering (Fig. 3). Among the less transparent regions were the ventricles and from ED18.5 also atria and all deeper structures, while surface structures such as coronary arteries were sufficiently well cleared for whole-mount imaging with confocal microscope.

The last and perhaps the most effective method for the embryos and embryonic hearts tested was the CUBIC protocol (Tainaka et al. 2014). CUBIC protocol is a gentle method, which does not result in pronounced shrinking or expansion of the tissue (Fig. 1). Moreover, GFP fluorescent signal was well preserved in all embryonic and adult stages studied. Even in stages older than ED12.5, the tissue was sufficiently transparent (Figs. 3, 4, 5) for observation with confocal microscope and OPT. CUBIC enabled us to observe not only superficial structures, such as coronary arteries (Fig. 4), but also deeper structures (ventricular trabeculae, branches of the basilar artery in the head and pectinate muscles (Figs. 2, 3). Its superiority relative to SCALE was especially noted in the deeper layers (Figs. 2, 3). Improved tissue transparency was also achieved through

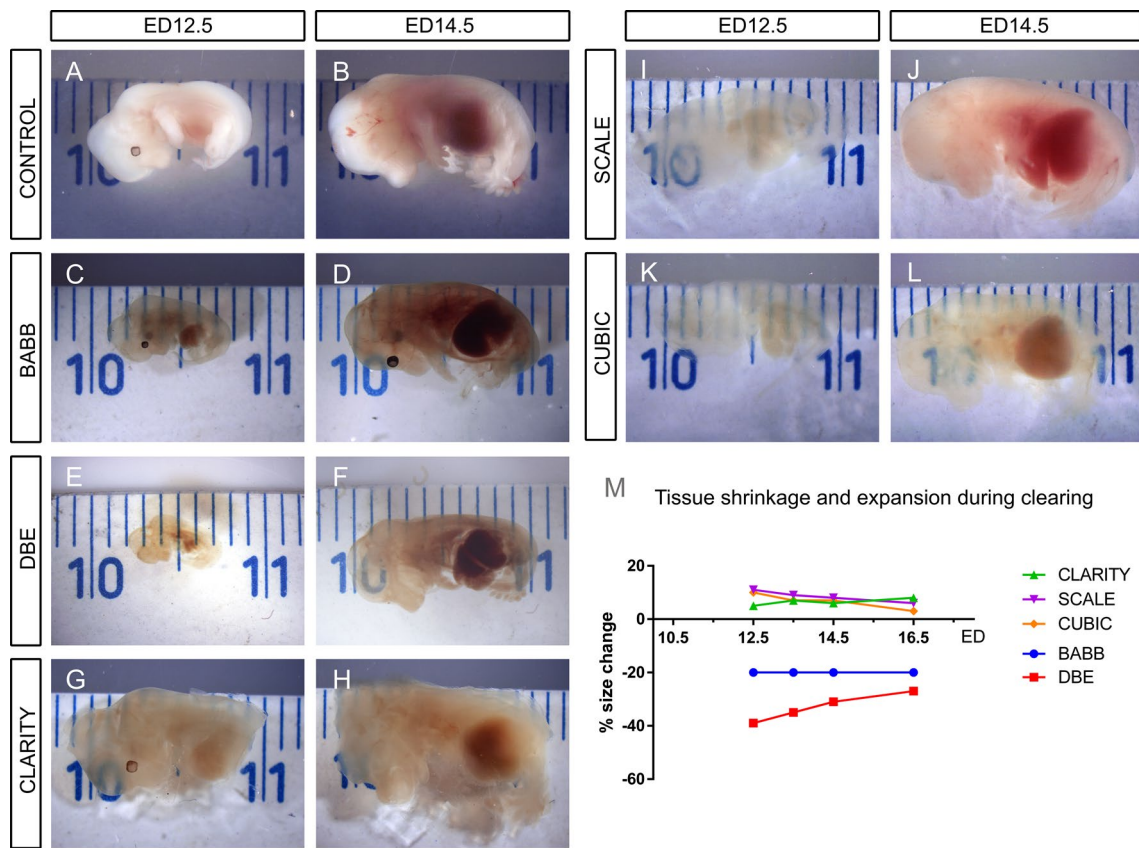


Fig. 1 Comparison of different tissue clearing protocols on early-stage (ED12.5) and later stage (ED14.5) whole embryos, processed in parallel. All embryos were fixed in 4 % paraformaldehyde and washed in PBS (control) and subsequently processed in different clearing methods. Note that both BABB (c, d) and DBE (e, f) cause considerable tissue shrinking compared to control (a, b), while CLARITY (g, h) and SCALE (i, j) result in specimen expansion (m). Some embryos have pigmented eyes, while the others are albinos (b, f, g–j), as neither tissue clearing protocol removes pigmen-

tation. While SCALE and CUBIC (i, j) work well for the younger stage, there is a notable difference at the later stage, with CUBIC being the best option. Note that the most opaque region is liver filled with blood. Panel m shows the tissue shrinkage and expansion during clearing for stages ED12.5, ED13.5, ED14.5 and ED16.5 processed with all methods tested. Measured as a difference in crown-rump length between fixation and clearing. Note that tissue shrinkage/expansion is most pronounced in the youngest embryos

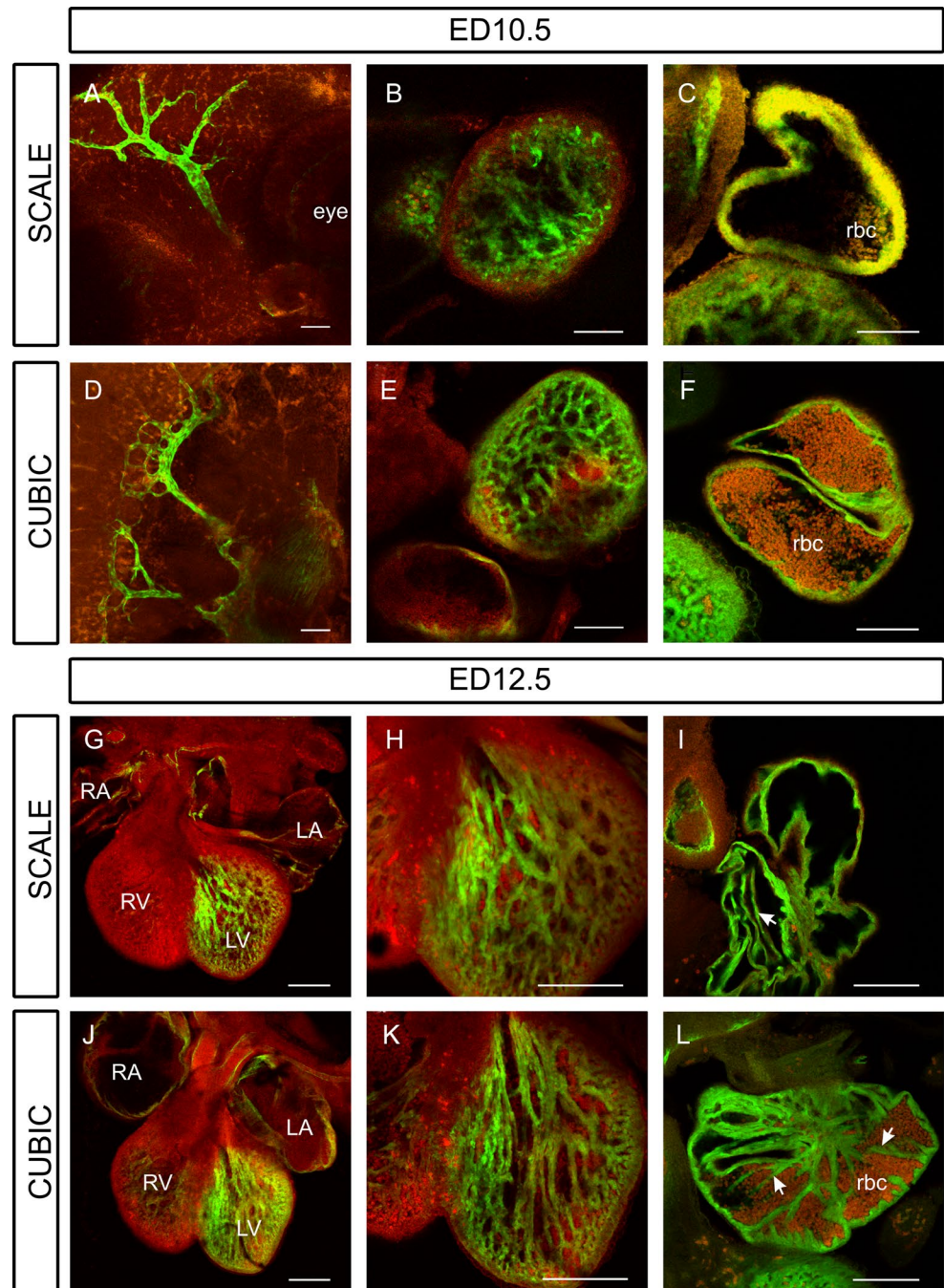
iron removal from the tissues. Embryo transparency was sufficient, according to the developmental stage, after 7–14 days in CUBIC, embryonic hearts were cleared after 5 days, and the adult hearts needed to be immersed in CUBIC for 30 days. Even after 1 month in CUBIC solution, the GFP fluorescence was preserved. We have modified the original Tainaka et al. (2014) CUBIC protocol and found that for the mouse embryos and hearts is sufficient to use CUBIC-1 protocol (here referred as CUBIC). There was no need to transfer the embryos to CUBIC-2 solution, as proposed by Tainaka et al. (2014). In general, the usable observation depth was over 2 mm, which was perfectly sufficient for our samples, as well as for the limits imposed by the imaging lenses (≤ 4 mm working distance).

Three-dimensional renderings using the OPT and SPIM techniques showed complete 3D images of the entire

sample—the whole embryo and isolated hearts (Fig. 5), which gave us the possibility to resolve macroscopic anatomical structures. Having general overview was advantageous compared to confocal microscope, which usually only provided field of view corresponding to the imaging lens, unless time-consuming image stitching was performed. Broader view was, however, offset by lower spatial resolution.

Maximum sample size for OPT is about 12 mm in diameter; however, due to more difficult clearing and light scattering in thick specimens, acquired data may be of low quality. Well-cleared specimens with sizes up to 5 mm in diameter appeared optimal. Maximum sample size for SPIM is about 4 mm in diameter, but due to using a 10 \times magnification objective, specimens 1–2 mm in diameter were more convenient and easier to capture.

Fig. 2 Comparison of confocal microscope images using SCALE and CUBIC protocols at early stages: ED10.5 (a–f) and ED12.5 (g–l). There is slightly better imaging of fine head vasculature in CUBIC (d) compared to SCALE (a). **a** is a maximum intensity projection (MIP) of a Z-stack of 24 slices, and **d** is a MIP of a Z-stack of 10 slices. Also fine structures of the younger embryo such as the trabeculae (b, e) and atria (c, f) are slightly better in CUBIC-cleared embryos. At older stage ED12.5, where trabeculae (g, h, j, k) and atria (i, l) are well formed, both techniques are yielding similar and satisfactory results. *Eye* embryonic eye, *LA* left atrium, *LV* left ventricle, *RA* right atrium, *RV* right ventricle, *rbc* red blood cells; *arrows* point to the forming pectinate muscles. *Scale bar* is 100 μ m in all images



Discussion

Comparison of the tissue clearing methods

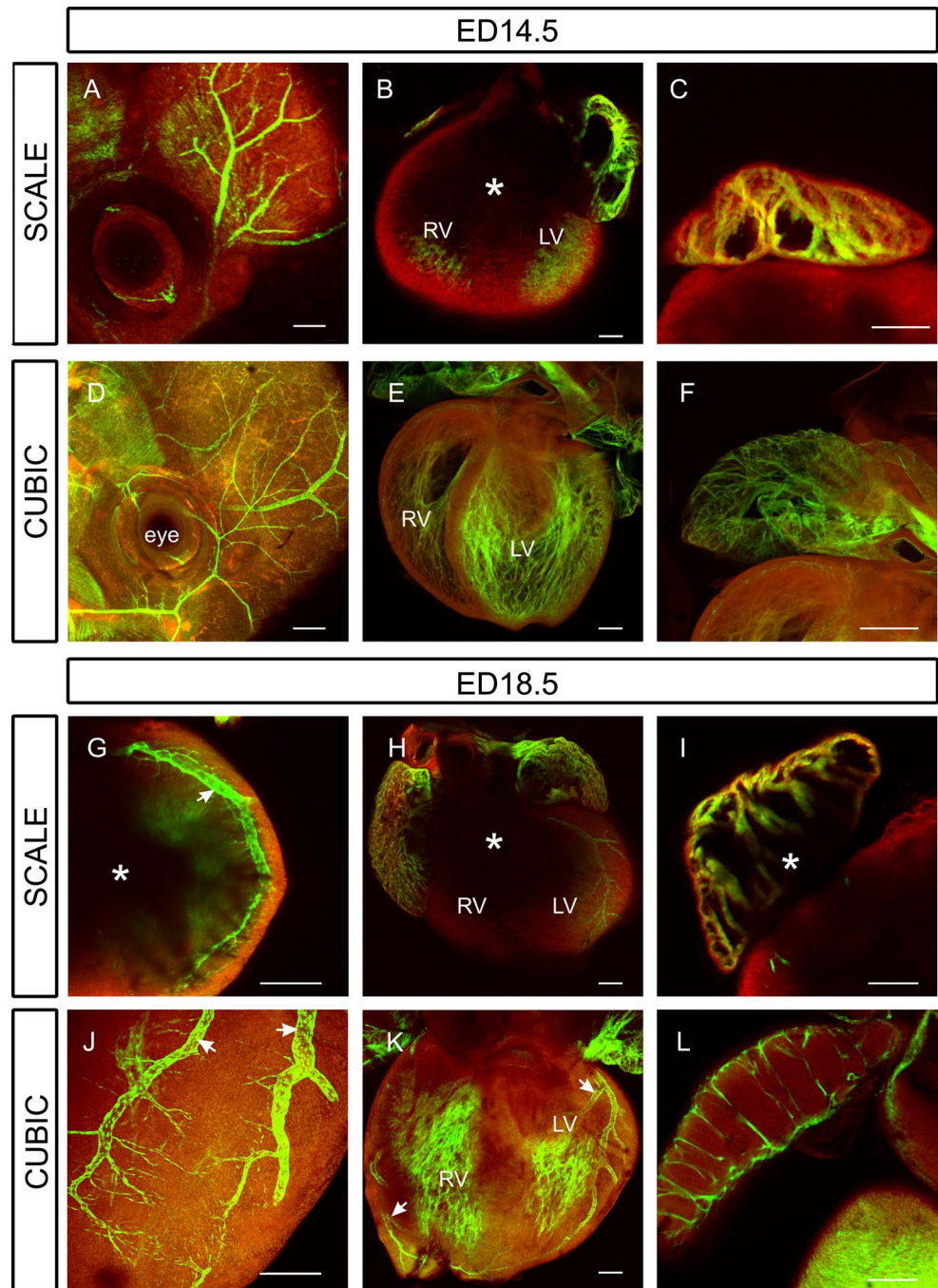
BABB is widely used tissue clearing method (Sivaguru et al. 2015), but it was previously known that it does not preserve GFP fluorescent signal and causes a considerable tissue shrinkage (Becker et al. 2012; Fig. 1; Table 1).

Surprisingly, DBE, an organic solvent-based tissue clearing method expected to preserve GFP signal (Becker

et al. 2012) did not preserve GFP fluorescence. It is possible, as the authors admitted (Erturk et al. 2012), that prolonged storage time resulted in an insufficient GFP signal. As sample storage is a requirement, other methods of tissue clearing and storage were evaluated.

Also CLARITY was suitable only for clearing adult hearts corresponding with published application for an adult fish, mouse and human brain (Chung et al. 2013; Tomer et al. 2014). It is possible that the embryonic tissues with higher water contents do not cross-link sufficiently to

Fig. 3 Comparison of confocal microscope images using SCALE and CUBIC protocols at later embryonic stages: ED14.5 (a–f) and ED18.5 (g–l). The better ability of the CUBIC protocol to clear matched specimens for whole-mount imaging becomes obvious. More detailed branches of basilar artery are visible in the CUBIC-cleared embryos (A: MIP of a Z-stack of 14 slices, D: MIP of a Z-stack of 12 slices). Note detailed resolution of the branching coronary arteries in the CUBIC embryos compared to imaging of superficial structures only in the SCALE embryos (G: MIP of a Z-stack of 23 slices, J: MIP of a Z-stack of 18 slices). CUBIC-treated embryos show well-resolved details of trabeculae, coronary arteries (E: single slice, K: MIP of a Z-stack of 17 slices) and atria (F: MIP of a Z-stack of 20 slices, L: single slice), while SCALE-treated embryos are not transparent enough to be able to show deeper structures (B: single slice, H: MIP of a Z-stack of 35 slices) or detailed atria (I: single slice, C: MIP of a Z-stack of 3 slices). *Eye* embryonic eye, *LA* left atrium, *LV* left ventricle, *RA* right atrium, *RV* right ventricle, *arrows* coronary arteries. *Asterisks* mark inadequately cleared regions. *Scale bar* 100 μ m



the gel, resulting in significant decrease of GFP fluorescent signal in mouse embryos.

SCALE tissue clearing method was also published on mouse brains (Hama et al. 2011), and unlike CLARITY, it can be used also for embryos and embryonic hearts. SCALE was not able to clear enough adult heart tissues as it does in brain (Hama et al. 2011); thus, only surface structures such as coronary arteries could be observed in detail.

The best tissue clearing method preserving GFP signal in embryonic hearts was CUBIC (Tainaka et al. 2014).

CUBIC is already well tested in adult whole-mount mouse heart, brain, muscles, liver, kidney, spleen and other organs (Tainaka et al. 2014). Here we expanded the use of CUBIC tissue clearing protocol also for mouse embryonic tissues, whole mouse embryos and hearts. Compared to other method tested, CUBIC cleared the tissue completely with removing iron ions as well; thus, the whole tissue volume could be observed with a confocal microscope, OPT or SPIM. CUBIC also enabled us to observe in detail structures such as branches of the basilar artery, coronary

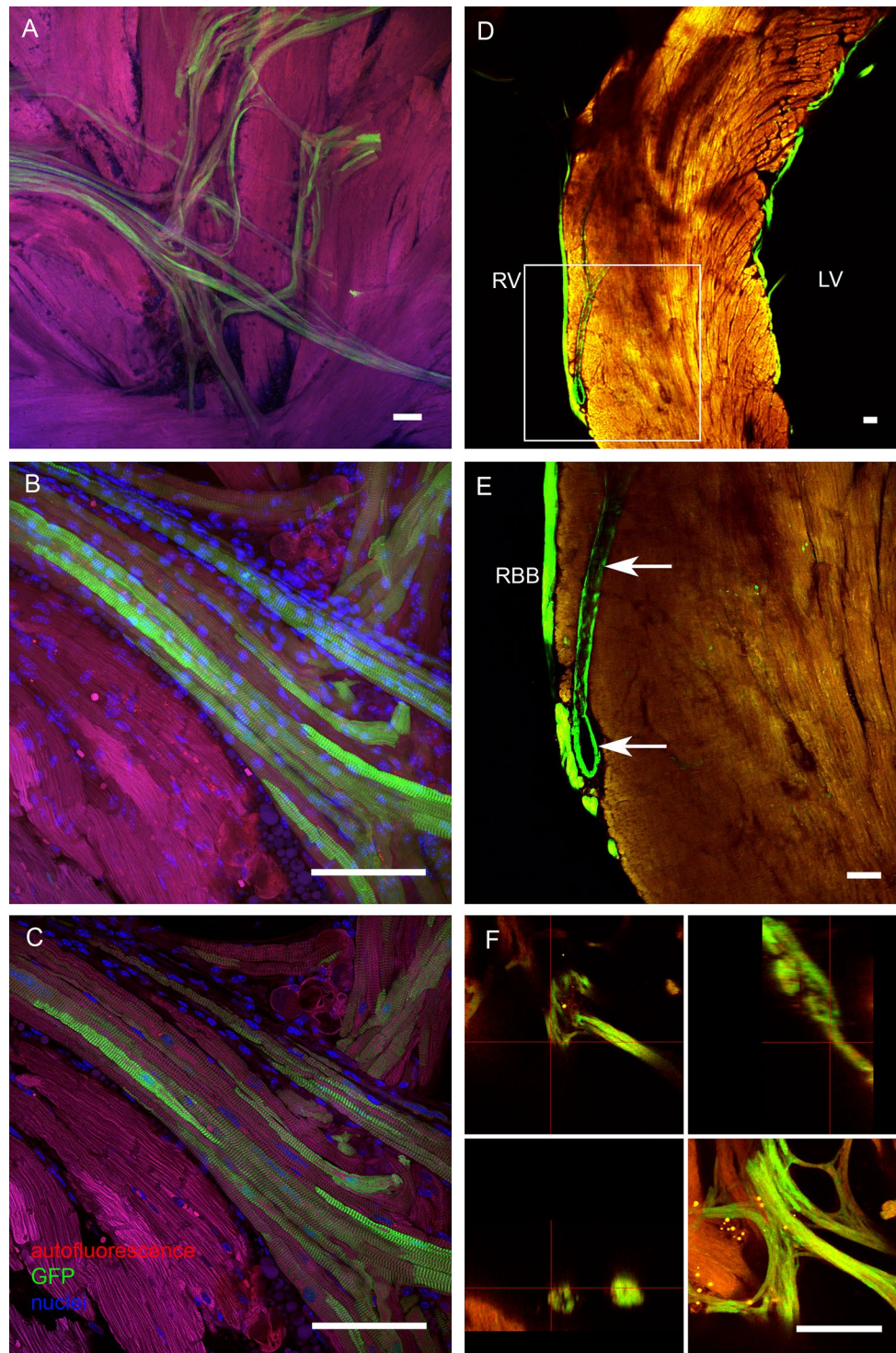


Fig. 4 Examples of SCALE, CLARITY and CUBIC protocols in the adult heart. **a–c** Confocal microscopy of SCALE-cleared specimens with nuclear counterstaining. **a** $\times 10$ objective MIP of 100-micron Z-stack showing the interior of the left ventricle with Purkinje fibers (*green*). **b** $\times 40$ oil immersion objective (1.3 NA) MIP of a 35-micron Z-stack. **c** Single optical section 20 μm deep with nuclear counterstain showing nuclei of the cardiomyocytes, allowing estimation of nucleation in sub-populations of conduction system (*green*) and working (*red*) myocytes. **d–e** CLARITY-cleared specimen. **d** shows a $\times 4$ view of the transverse section of the interventricular septum.

GFP fluorescence is preserved, labeling both the coronary artery endothelium (**e** taken with $\times 10$ objective, *arrow*) and subendocardially located conduction myocytes of the right bundle branch. **f** 3D visualization of a stack acquired with $\times 25$ ScaleView objective showing in orthogonal views and maximum intensity projection details of the Purkinje network. Cleared with CUBIC. For more examples of 3D imaging using this $\times 25$ lens, please see the Supplemental Movies 3–5. *LV* left ventricle, *RV* right ventricle, *RBB* right bundle branch, *arrows* coronary artery, *scale bars* 100 μm

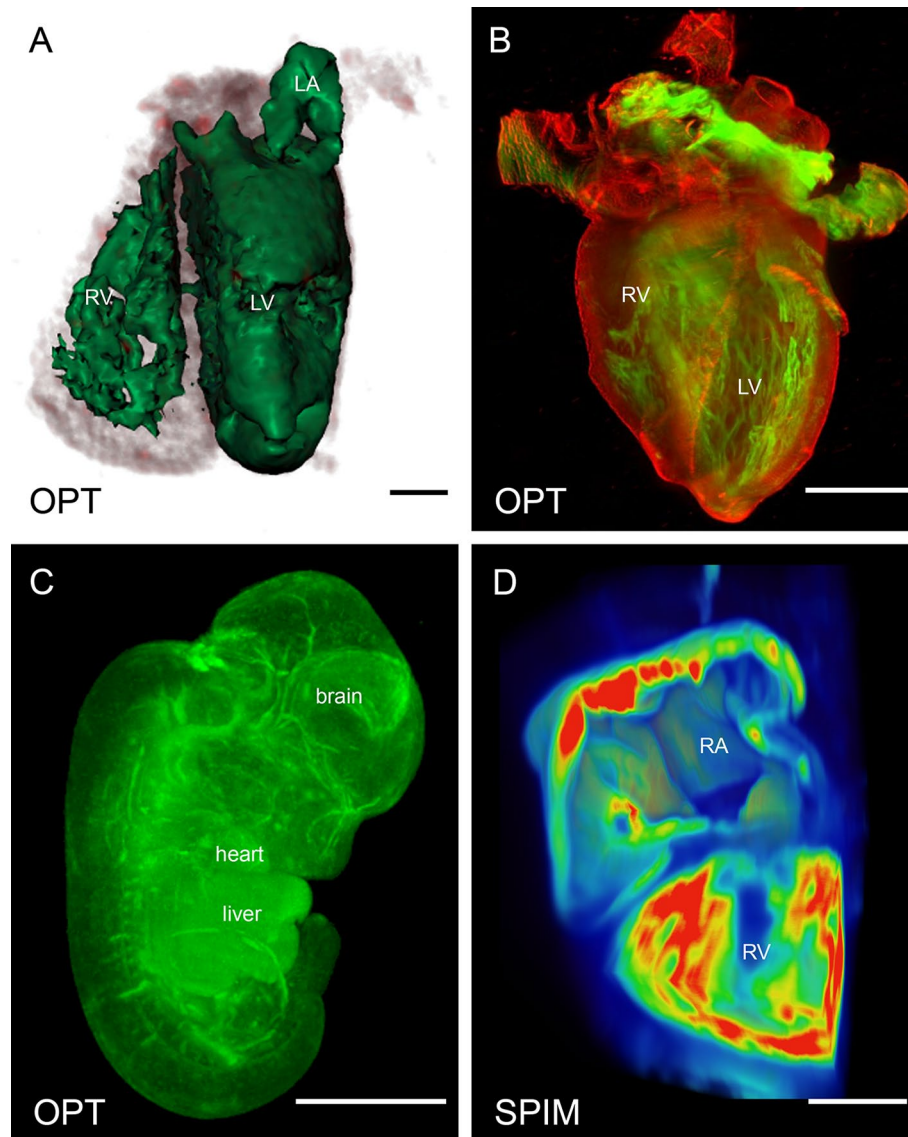


Fig. 5 3D visualization techniques. 3D visualizations of specimens cleared by various techniques, acquired and visualized by an OPT microscope and VolViewer software package, Bangham laboratory (**a–c**) and a SPIM and Amira 3D, FEI software (**d**), respectively. **a** ED12.5 mouse heart with a scissor cuts through the right ventricle, BABB clearing, primary antibody against GFP detected with Cy5-coupled secondary. Red–gray channel is transmission one, and green channels is isosurface rendering of the fluorescent channel acquired using excitation of 628/40 nm and emission of 692/40 nm. Scale bar 200 μ m. **b** ED16.5 mouse heart with a scissor cuts through both ventricles, SCALE clearing. Maximum intensity projection (MIP) visualization of overlays of red (transmission) channel and green (fluorescent) channel using excitation of 425/40 nm and emission of 475 nm

(high pass). GFP-positive network of Purkinje fibers is clearly visible. For full view, please see the Supplemental Movie 1. Scale bar 850 μ m. **c** ED12.5 mouse embryo cleared in CUBIC. MIP visualization of fluorescent channel using excitation of 425/40 nm and emission of 475 nm (high pass). GFP positivity is seen in the head arteries and heart; lot of autofluorescence is apparent in the liver. For full view, please see the Supplemental Movie 2. Scale bar 2 mm. **d** ED12.5 mouse heart with a virtual cuts through the right atrium and ventricle. Strong GFP signal (shown in red with the pseudocolor display) is visible in the pectinate muscles of the atrium and ventricular trabeculae. Cleared in CUBIC. Scale bar 200 μ m. LA left atrium, LV left ventricle, RA right atrium, RV right ventricle

arteries, fine structure of ventricular trabeculae and pectinate muscles. According to the original description (Tainaka et al. 2014), CUBIC is also suitable for tissue clearing after immunolabeling and preserves well fluorescent anti-body signal.

Our study compares five different tissue clearing methods based on their ability to render the mouse embryo and heart transparent and to preserve GFP signal. As image acquisition and processing allow to compensate for fluorescent signal decline with depth, which can up to certain

Table 1 Main advantages and disadvantages of clearing protocols tested in this study

	Ease, speed (for embryo ED16.5)	Hazards	Positives	Negatives
B/ABB	One-day, easy protocol (with rocking)	Strong solvent, benzyl alcohol and benzyl benzoate	Undemanding protocol, good tissue transparency	Does not preserve GFP, dissolves plastic, must be held in glass vessels, tissue shrinkage
DBE	One-day protocol	Tetrahydrofuran, dibenzylether	Rapid protocol, good clearing	Does not preserve GFP, tissue shrinkage
CLARITY	Long protocol, 5-day electrophoresis, 1 week further clearing with SCALE	Acrylamide—highly toxic	Further improved tissue transparency, possible whole-mount immunohistochemistry	Partial loss of GFP, demanding protocol, requires custom-made equipment
SCALE	Easy, 2 weeks in SCALE with regular changes	Urea, glycerol, Triton X	Undemanding protocol, preserves well GFP	Incomplete transparency, tissue expansion
CUBIC	Easy, 2 weeks in CUBIC1 with rocking and solution changes	N,N,N'-tetrakis(2-hydroxypropyl)ethylenediamine, urea, Triton X	Undemanding protocol, good GFP preservation, best tissue transparency, both superficial and deep structures visible	Mild tissue expansion, slightly different refractive index from SCALE

level compensate less than ideal tissue transparency, our results are not quantitative as the recent study of Hama et al. (2015), but assess instead the ability of each method to produce quality data and images. None of the methods removes the dark pigmentation of the eye, making it a useful marker for orientation and evaluation of transparency; if detailed study of the eye is important, then albino strains should be used for the studies.

Imaging

Single-photon confocal microscopy is a well-known method for 3D observation of embryonic tissues stained whole mount. When combined with a suitable tissue clearing protocol, it enables us to observe detailed structures on the surface as well as deep in the embryo. Clear tissue can be reconstructed to render its entire 3D structure, without a need of physical sectioning. Imaging depth and clarity can be further improved by two-photon excitation (Supplemental Movie 1 and 2), as we showed already in Miller et al. (2005); however, due to its costs, two-photon excitation is not universally available on all systems. The resolution limit is the most apparent in the Z-axis; in general, there is a trade-off between the desire for the maximal numerical aperture (critical for Z-resolution) and working distance (high numerical aperture requires short working distance, which significantly limits the depth of imaging). For example, while the 4× objective lens with NA 0.16 has working distance of more than 1 cm, the high-resolution 40× oil immersion lens with NA 1.3 is not able to image deeper than 200 μm. One of the solutions for this problem is the specifically designed ScaleView lens, available from Olympus (25×, with NA 1.0 and WD 4 mm, or 0.9 and 8 mm) or Zeiss (20×, NA 1.0, WD 5 mm), which allows collection of large Z-stacks at resolution of 1 micron or less (Hama et al. 2011). The only practical difficulties with this objective are its size (non-standard diameter necessitating a different objective mount, length requiring re-arrangement of the stage to accommodate it) and high price. For observation, we found it necessary to locate the region of interest first using a dry, low NA, long working distance 4× lens, since it was almost impossible to discern any structure in the epifluorescence wide-field mode due to the high NA of the 25× objective and resulting brightness.

Both confocal laser scanning microscopy and OPT/SPIM can be considered as complementary techniques for 3D visualization of specimens. OPT/SPIM allows acquisition of data with proper morphological and spatial information of whole specimens, up to several millimeters of diameter, without the necessity to cut the specimens and without deformations introduced by the cutting. Obtained resolution is low (>20 μm/pixel); thus, OPT/SPIM enables

us to see global anatomical structures of the specimens. On the contrary, resolution of confocal microscope is much higher (up to 200 nm/pixel), which provides high-resolution insight into subtle structures of specimens, albeit in a restricted field of view only. When large specimens are visualized by a confocal microscope, acquisition of multiple overlapping fields of view and their stitching may be required. The complete image of the heart can be created using volume reconstruction methods (Capek et al. 2009). Thus, in practice, up to ED10.5 the confocal microscopy is the better choice for whole embryo; higher detail can be obtained from superficially positioned regions of interest such as the heart with a dry 20 \times , 0.75 NA, WD 0.6 mm objective. For more advanced stages, OPT is more suitable for whole embryos or whole hearts past ED11.5.

In conclusion, from the tested methods the CUBIC protocol appeared to be the best for whole-mount GFP cardiac samples. SCALE technique was also found suitable for younger embryos. The imaging method of single-photon confocal microscopy was well complemented with the OPT. In the future, these protocols will be used for three-dimensional reconstructions of normal and abnormal specimens to visualize the developing cardiac conduction system and coronary vasculature.

Acknowledgments We would like to thank Ms. Alena Kvasilova and Klara Krausova for their excellent technical assistance. We are grateful to Prof. Paul Mozdziak for his kind editing of the English usage and helpful criticism. This study was supported by 13-12412S from the Czech Science Foundation, Ministry of Education PRVOUK P35/LF1/5, institutional support RVO:67985823, AMVIS LH13028 and Charles University UNCE 204013.

Compliance with ethical standards

Conflict of interest The authors declare that they have no conflict of interest.

References

- Becker K, Jahrling N, Saghati S, Weiler R, Dodt HU (2012) Chemical clearing and dehydration of GFP expressing mouse brains. *PLoS ONE* 7:e33916
- Biben C, Weber R, Kesteven S, Stanley E, McDonald L, Elliott DA, Barnett L, Koentgen F, Robb L, Feneley M, Harvey RP (2000) Cardiac septal and valvular dysmorphogenesis in mice heterozygous for mutations in the homeobox gene *Nk2-5*. *Circ Res* 87:888–895
- Capek M, Bruza P, Janacek J, Karen P, Kubinova L, Vagnerova R (2009) Volume reconstruction of large tissue specimens from serial physical sections using confocal microscopy and correction of cutting deformations by elastic registration. *Microsc Res Tech* 72:110–119
- Chung K, Wallace J, Kim SY, Kalyanasundaram S, Andalman AS, Davidson TJ, Mirzabekov JJ, Zalocusky KA, Mattis J, Denisin AK, Pak S, Bernstein H, Ramakrishnan C, Grosenick L, Gradinaru V, Deisseroth K (2013) Structural and molecular interrogation of intact biological systems. *Nature* 497:332–337
- Cvetko E, Capek M, Damjanovska M, Reina MA, Erzen I, Stopar-Pintaric T (2015) The utility of three-dimensional optical projection tomography in nerve injection injury imaging. *Anaesthesia* 70:939–947
- Erturk A, Becker K, Jahrling N, Mauch CP, Hojer CD, Egen JG, Helal F, Bradke F, Sheng M, Dodt HU (2012) Three-dimensional imaging of solvent-cleared organs using 3DISCO. *Nat Protoc* 7:1983–1995
- Hama H, Kurokawa H, Kawano H, Ando R, Shimogori T, Noda H, Fukami K, Sakaue-Sawano A, Miyawaki A (2011) Scale: a chemical approach for fluorescence imaging and reconstruction of transparent mouse brain. *Nat Neurosci* 14:1481–1488
- Hama H, Hioki H, Namiki K, Hoshida T, Kurokawa H, Ishidate F, Kaneko T, Akagi T, Saito T, Saido T, Miyawaki A (2015) ScaleS: an optical clearing palette for biological imaging. *Nat Neurosci* 18:1518–1529
- Hu N, Sedmera D, Yost HJ, Clark EB (2000) Structure and function of the developing zebrafish heart. *Anat Rec* 260:148–157
- Jouk PS, Usson Y, Michalowicz G, Grossi L (2000) Three-dimensional cartography of the pattern of the myofibres in the second trimester fetal human heart. *Anat Embryol (Berl)* 202:103–118
- Ke MT, Fujimoto S, Imai T (2013) SeeDB: a simple and morphology-preserving optical clearing agent for neuronal circuit reconstruction. *Nat Neurosci* 16:1154–1161
- Miller CE, Thompson RP, Bigelow MR, Gittinger G, Trusk TC, Sedmera D (2005) Confocal imaging of the embryonic heart: how deep? *Microscop Microanal* 11:216–223
- Miquerol L, Meysen S, Mangoni M, Bois P, van Rijen HV, Abran P, Jongsma H, Nargeot J, Gros D (2004) Architectural and functional asymmetry of the His-Purkinje system of the murine heart. *Cardiovasc Res* 63:77–86
- Pitrone PG, Schindelin J, Stuyvenberg L, Preibisch S, Weber M, Eliceiri KW, Huiskens J, Tomancak P (2013) OpenSPIM: an open-access light-sheet microscopy platform. *Nat Methods* 10:598–599
- Ryu S, Yamamoto S, Andersen CR, Nakazawa K, Miyake F, James TN (2009) Intramural Purkinje cell network of sheep ventricles as the terminal pathway of conduction system. *Anat Rec (Hoboken)* 292:12–22
- Sankova B, Benes J Jr, Krejci E, Dupays L, Theveniau-Ruissy M, Miquerol L, Sedmera D (2012) The effect of connexin40 deficiency on ventricular conduction system function during development. *Cardiovasc Res* 95:469–479
- Sedmera D, Pexieder T, Hu N, Clark EB (1997) Developmental changes in the myocardial architecture of the chick. *Anat Rec* 248:421–432
- Sharpe J, Ahlgren U, Perry P, Hill B, Ross A, Hecksher-Sorensen J, Baldock R, Davidson D (2002) Optical projection tomography as a tool for 3D microscopy and gene expression studies. *Science* 296:541–545
- Simon AM, Goodenough DA, Paul DL (1998) Mice lacking connexin40 have cardiac conduction abnormalities characteristic of atrioventricular block and bundle branch block. *Curr Biol* 8:295–298
- Sivaguru M, Fried G, Sivaguru BS, Sivaguru VA, Lu X, Choi KH, Saif MT, Lin B, Sadayappan S (2015) Cardiac muscle organization revealed in 3-D by imaging whole-mount mouse hearts using two-photon fluorescence and confocal microscopy. *Bio-techniques* 59:295–308
- Tainaka K, Kubota SI, Suyama TQ, Susaki EA, Perrin D, Ukai-Tadenuma H, Ukai H, Ueda HR (2014) Whole-body imaging with single-cell resolution by tissue decolorization. *Cell* 159:911–924
- Tomer R, Ye L, Hsueh B, Deisseroth K (2014) Advanced CLARITY for rapid and high-resolution imaging of intact tissues. *Nat Protoc* 9:1682–1697

- Zhao X, Wu J, Gray CD, McGregor K, Rossi AG, Morrison H, Jansen MA, Gray GA (2015) Optical projection tomography permits efficient assessment of infarct volume in the murine heart postmyocardial infarction. *Am J Physiol Heart Circ Physiol* 309:H702–H710
- Zucker RM, Hunter S, Rogers JM (1998) Confocal laser scanning microscopy of apoptosis in organogenesis-stage mouse embryos. *Cytometry* 33:348–354